Journal of
Computational and Theoretical Nanoscience
Vol. 6, 1320–1327, 2009

Sequential H_2 Chemisorption and H Desorption on Icosahedral Pt_{13} and Pd_{13} Clusters: A Density Functional Theory Study

Chenggang Zhou[1], Shujuan Yao[1], Jinping Wu[1], Liang Chen[2], Robert R. Forrey[3], and Hansong Cheng[4,*]

[1] *Institute of Theoretical Chemistry and Computational Materials Science, China University of Geosceinces Wuhan, Wuhan 430074, China*
[2] *Ningbo Institute of Materials Technology and Engineering, Chinese Academy of Sciences, Ningbo, Zhejiang 315201, China*
[3] *Penn State University, Berks-Lehigh Valley College, Reading, PA 19610-6009, USA*
[4] *Air Products and Chemicals, Inc. 7201 Hamilton Boulevard, Allentown, PA 18195-1501, USA*

We present a density functional theory (DFT) study on the sequential H_2 dissociative chemisorption and H desorption on icosahedral Pt_{13} and Pd_{13} clusters. The coverage dependence of the sequential adsorption and desorption energies are given along with the charge transfer from metals to H. At low H coverage, the dissociation takes place at an atop site before diffusion redistributes the atoms to well-separated edge sites. At higher coverage, the edge sites become filled and the cluster undergoes a structure-transition from icosahedral to an *fcc*-like structure (these transitions occur at 10 H atoms for Pt_{13} and 24 H atoms for Pd_{13}). Upon further H loading, the dissociated H atoms may reside at the cluster surface or be pulled inside to interact with the core metal atom. *Ab initio* molecular dynamics simulation and bond-distance distribution analysis shows that H-saturation occurs at 44 H atoms for Pt_{13} and 30 H atoms for Pd_{13}. The calculated H_2 dissociative chemisorption energy and H desorption energy at saturation is 0.90 eV and 2.02 eV for Pt_{13}, and 0.76 eV and 2.04 eV for Pd_{13}, respectively. These values are comparable with what was reported for smaller close-packed clusters, which suggests that the catalytic performance of these transition metal clusters may not vary significantly with particle size or shape but instead depends primarily on the available surface metal atoms which can be accessed by H atoms.

Keywords: Icosahedral Clusters, H_2 Dissociative Chemisorption, Sequential H Desorption, Saturation.

RESEARCH ARTICLE

1. INTRODUCTION

Hydrogen dissociative chemisorption on precious transition metal catalysts such as Pt and Pd is of great industrial importance in various hydrogenation/dehydrogenation and electrocatalysis processes.[1–4] In these reactions, hydrogen molecules are dissociated with active hydrogen atoms adsorbed on the catalyst surfaces. Understanding the elementary processes of these chemical reactions is essential for design and development of novel catalysts to achieve high catalytic efficiency. Unfortunately, a detailed atomic scale knowledge of sequential dissociative adsorption on metal cluster catalysts under realistic conditions of constant flow of gaseous hydrogen remains limited.

The interaction between hydrogen and metal surfaces has been investigated extensively using both experimental[5–19] and theoretical methods[20–26] in order to understand the reactivity of hydrogen with the metal atoms and the nature of the bonds. For Pt(111) and Pd(111) surfaces, the maximum adsorption energy of a single hydrogen atom was calculated to be 0.46 eV and 0.51 eV, respectively with a reaction barrier that is lower on the Pt surface than on the Pd surface.[24] Experimental studies using thermal desorption spectroscopy reported that the adsorption energy per H_2 dissociating on Pt(111) lies within the range 0.70 to 0.83 eV.[5–10] Theoretical calculations found the binding energy of one H_2 molecule adsorbed on the Pt(111) surface

*Author to whom correspondence should be addressed.

 1546-1955/2009/6/1320/008 doi:10.1166/jctn.2009.1181

to be 0.80 eV in good agreement with the experimental results.[23]

The chemical reactivity of H_2 on clusters is normally much higher than on crystalline surfaces due to finite size effects introduced by sharp corners and edges. Balasubramanian and co-workers calculated H_2 dissociative chemisorption energy on Pt_2 and Pt_3 clusters using multi-configuration self-consistent field theory (MCSCF) and reported a value of 0.93–1.33 eV.[27,28] Using X-ray absorption spectra together with DFT calculations, it was found that the binding energy of two hydrogen atoms on F_2O and Na_2O supported Pt_4 clusters is 0.74 eV and 0.80 eV, respectively.[17] From H/D desorption experiments, the binding energy for H_2 on a Pt_{13} cluster supported by NaY zeolite was found to be somewhat larger with a reported value of 1.36 eV.[18] Other calculations reported a chemisorption energy of 1.40 eV for H_2 dissociatively adsorbed at the on-top site of *fcc* Pt_{13} cluster[29–31] and 0.64–1.50 eV for unsupported Pt_{13} clusters with various amounts of H coverage.[18] Clearly, it would be desirable to have a detailed understanding of all factors that influence the chemical reactivity of the clusters such as the size and shape of the cluster, the active bonding sites, the amount of H coverage, and the role of the cluster support.

In previous work, we investigated the nature of the hydrogen sequential adsorption on small platinum and palladium clusters.[32–34] For Pt_n ($n = 2$–9) clusters, we found that the chemisorption energies, which ranged from 1.4 eV to 1.8 eV at low H coverage, decreased to ~0.9 eV at full saturation, while the sequential desorption energies, which ranged from 2.8 eV to 3.2 eV at low coverage, decreased to ~2.5 eV at saturation.[32,33] For Pd_n ($n = 2$–9) clusters, the chemisorption and desorption energies again decreased with H coverage, and at saturation were found to be 0.6–0.8 eV and 2.3–2.7 eV, respectively.[34] All adsorption energies are larger on these clusters than on the corresponding (111) surfaces. Therefore, we expect that nano-size transition metal clusters would have higher chemical reactivity compared to flat transition metal surfaces. For both Pt_n and Pd_n, the saturation values were within a limited range which suggests that these critical energies may be insensitive to cluster size and configuration. It is desirable to see whether this trend continues for larger clusters that may be important for realistic catalytic systems.

It is also noteworthy that the magnetic moments for all of the small Pt and Pd clusters that we studied previously were found to vanish at full H saturation.[32–36] A recent experiment conducted by Liu et al.[18] on an icosahedral Pt_{13} cluster residing in an NaY zeolite, however, found that the cluster remains paramagnetic upon H_2 dissociative chemisorption. They concluded that the cluster could bind up to 30 H atoms onto the surface, which is a considerably smaller H/Pt ratio than was found for the smaller Pt clusters. It was speculated that the non-vanishing magnetic moment and the relatively small H capacity of the cluster were both a consequence of inaccessible Pt–H bonds which leave unpaired $5d$ electrons.[29,30] This assumes that the cluster maintains its original structure throughout the H loading and that all interactions occur on the surface. A quantitative study is needed to determine whether the icosahedral symmetry of the cluster is stable as H coverage increases and whether the H atoms are able to penetrate into the core of the cluster.

In this work, we extend our previous investigations to include icosahedral Pt_{13} and Pd_{13} in order to understand their catalytic activity towards hydrogen. Unlike the smaller close-packed clusters, these icosahedral clusters possess a highly symmetric core–shell character, with 12 shell atoms and 1 core atom. We first locate the site preference of hydrogen atoms adsorbed on the Pt_{13} and Pd_{13} clusters as a function of coverage. Adsorption, diffusion and desorption of hydrogen are considered and careful attention is paid to structural rearrangements that may occur with increased H loading. We also investigate the dynamical behavior of hydrogen on the clusters in order to locate the saturation limit. The aim of this paper is to characterize the hydrogen interactions with icosahedral Pt and Pd clusters at full H coverage to determine the catalytic properties of these transition metal clusters and to see whether these clusters follow the trend found for smaller close-packed clusters where the saturation energies are not sensitive to cluster size and shape.

2. COMPUTATIONAL DETAILS

Our calculations were carried out using DFT under the generalized gradient approximation (GGA) with the Perdew-Wang's exchange-correlation functional[37,38] and a spin-polarized scheme. The effective core pseudopotential (ECP) was utilized to describe the core electrons and a double numerical basis set augmented with polarization function (DNP) was employed to describe the valence electrons. The energy and gradient convergence tolerance was chosen to be 2×10^{-5} Ha and 4×10^{-3} Ha/Å respectively. All structures were fully optimized to the energetically most stable configurations using conjugated gradient algorithm without symmetry constrains. The LST/QST method[39] was used to determine the transition state of H_2 dissociative chemisorption and diffusion on the Pt_{13} and Pd_{13} clusters. *Ab initio* molecular dynamics (MD) simulations and bond-distance distribution analysis were performed for each cluster size to determine possible structural rearrangements and the H saturation point. The *ab initio* MD simulations were run for 2 ps with a time step of 1 fs using a NVT ensemble with the temperature controlled by Nosé-Hoover chain thermostat under 300 K. All calculations were implemented in DMol^3 package.[40,41] The Hirshfeld population analysis was performed to evaluate the charge transfer from metal to H. The H_2 dissociative

RESEARCH ARTICLE

chemisorption energy ΔE_{CE} and the H sequential desorption energy ΔE_{DE} are defined by

$$\Delta E_{CE} = -\frac{2}{n}\left(E_{M_{13}H_n} - E_{M_{13}} - \frac{n}{2}E_{H_2}\right) \quad (1)$$

$$\Delta E_{DE} = E_H - \frac{1}{2}\left(E_{M_{13}H_n} - E_{M_{13}H_{n-2}}\right) \quad (2)$$

where n is the number of H atoms. $E_{M_{13}H_n}$ is the energy of $M_{13}H_n$ metal hydride, $E_{M_{13n}}$ is the energy of the bare metal cluster, and E_{H_2} is the energy of H_2 molecule.

3. RESULTS AND DISCUSSION

3.1. H_2 Reactions with Pt_{13} Icosahedral Cluster

Previous studies have shown that H_2 molecules readily dissociate on flat Pt surfaces[23,24] and on the surface of Pt clusters[29,30,32–34] yielding H atoms with high surface mobilities.[23,24,32–34] In the present study, we consider the highly symmetric Pt_{13} icosahedral structure and investigate the chemisorption of H_2 molecules on the cluster as a function of H coverage. We begin with a single H_2 molecule interacting with the bare cluster at one of three possible sites: 1-fold atop, 2-fold edge and 3-fold hollow of the Pt_{13} icosahedron. The calculated adsorption energy on these three sites is 1.37 eV, 1.46 eV and 1.21 eV, respectively, demonstrating that the edge site of icosahedral Pt_{13} is chemically the most active, in agreement with DFT/GGA results by Liu et al.[18] However, detailed frontier orbital analysis shows that the HOMO of Pt_{13} ($5d$) icosahedron has the largest overlap with the LUMO of $H_2(1s)$ at the atop site. Consequently, we further calculated the transition state (TS) of H_2 dissociation and H diffusion around the cluster with the H_2 molecule initially physisorbed at the atop site as shown in Figure 1. The dissociation of H_2 is nearly barrierless (TS1, 0.06 eV) yielding an initial product (P1) chemisorption energy of 1.05 eV. The H diffusion barriers (TS2 and TS3) are both less than 0.34 eV and the final product (P3) has a chemisorption energy of 1.65 eV with the two H atoms well-separated at the edge sites. This result confirms that H_2 dissociation and H diffusion occur easily on an icosahedral Pt_{13} cluster, and the energetically favorable accommodation is the edge site.

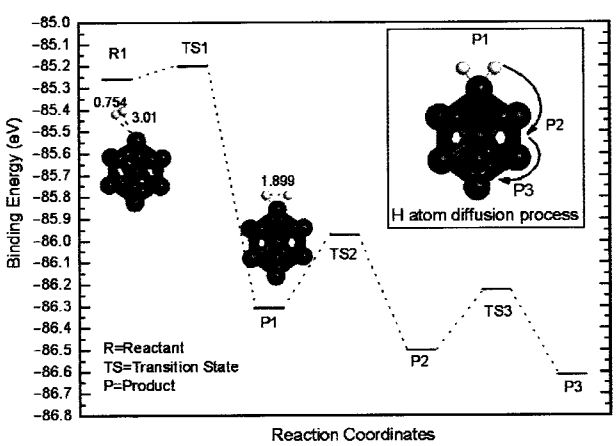

Fig. 1. The H_2 activation, dissociation and H diffusion pathway around the Pt_{13} cluster.

We then sequentially add H atoms onto the edge sites of the Pt_{13} cluster and fully optimize each structure until we find the energetically most favorable configuration. A few selected configurations are displayed in Figure 2(a). All of these configurations were verified by MD simulation to determine whether the system has reached H saturation. It was observed from the MD trajectories that the saturation point occurs at $n = 44$. For larger n, two H atoms are readily squeezed out from the cluster forming an H_2 molecule which is subsequently physisorbed onto the cluster surface. Figure 2(b) compares the H–H distance distributions for $Pt_{13}H_{44}$ and $Pt_{13}H_{46}$ and shows the peak at 0.74 Å for $n = 46$ which corresponds to the recombined H_2 molecule.

Figure 3(a) shows three distinct stages for sequential H loading on Pt_{13}. In the icosahedron stage, the average Pt–Pt bond distance increases rapidly with the number of H atoms, confirming that the sequential adsorption of H atoms causes an expansion of the Pt_{13} cluster at low H loading.[17,18] During this stage, the icosahedral symmetry of the Pt cluster is maintained and the most stable configurations all adopt a symmetric H–H pair distribution until $n = 8$. At $n = 10$, the Pt_{13} icosahedron encountered a sudden distortion to an *fcc*-like structure (Fig. 2(a3)). To ensure it is not an artifact, we performed MD simulation for 2 ps for $Pt_{13}H_8$ and the icosahedral shape was preserved. We then added two H atoms onto the edge sites of the $Pt_{13}H_8$ hydride and ran MD again for 2 ps. The energy evolution curve and the average Pt–Pt bond distance change with respect to dynamic steps are shown in the upper and lower panels of Figure 3(b), respectively. At the initial period of the MD simulation, only thermal motion of Pt and H atoms was observed. However, compared with $Pt_{13}H_8$, four additional Pt–H bonds are formed which weaken the Pt–Pt bonds resulting in a geometric instability. Consequently, the icosahedral symmetry is broken and the icosahedron makes a transition to an *fcc*-like configuration (this occurs around 1 ps in Fig. 3(b)). Further H loading follows the second stage of Figure 3(a) where each H atom is adsorbed onto the surface of the *fcc*-like cluster. The active edge sites are filled sequentially until all are occupied at $n = 24$ as shown in Figure 2(a4).

Two types of 4-membered H rectangles emerge at $n = 24$. One type has a Pt atom in the plane center whereas the other type has no central Pt atom. We name these the Pt@H_4 and Vac-H_4 sites, respectively. Our calculations found that the adsorption energy at the Pt@H_4 site is 0.12 eV higher than at the Vac-H_4 site, which was calculated to be −1.41 eV. Therefore, the Pt@H_4 sites are filled

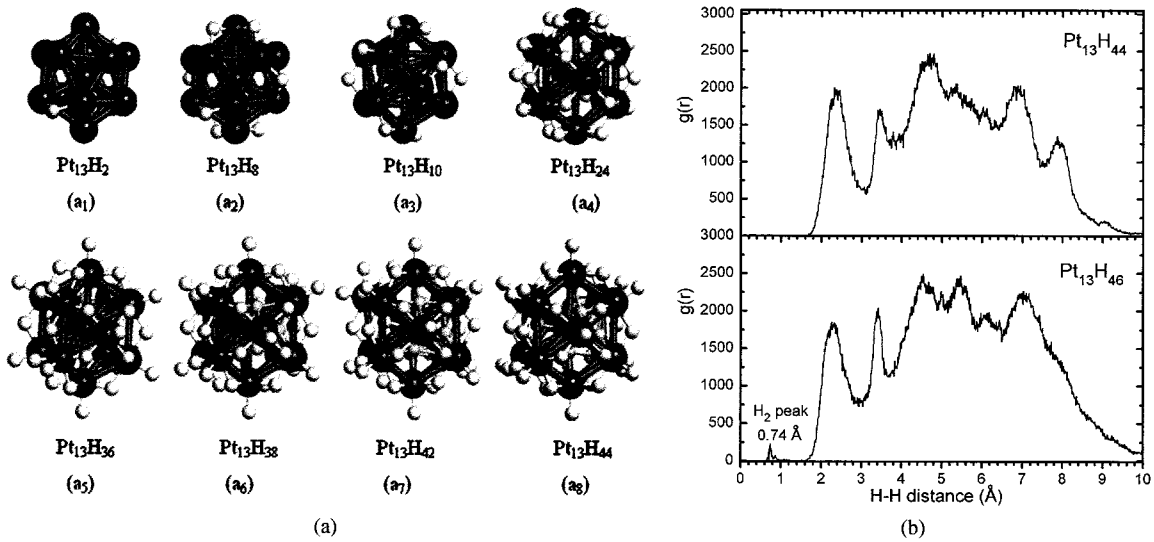

Fig. 2. (a) Optimized structures of H_2 sequential dissociative chemisorption on Pt_{13} cluster. Surface H atoms are shown in white and inside H atoms in yellow; (b) The calculated H–H distance distributions of $Pt_{13}H_{44}$ and $Pt_{13}H_{46}$.

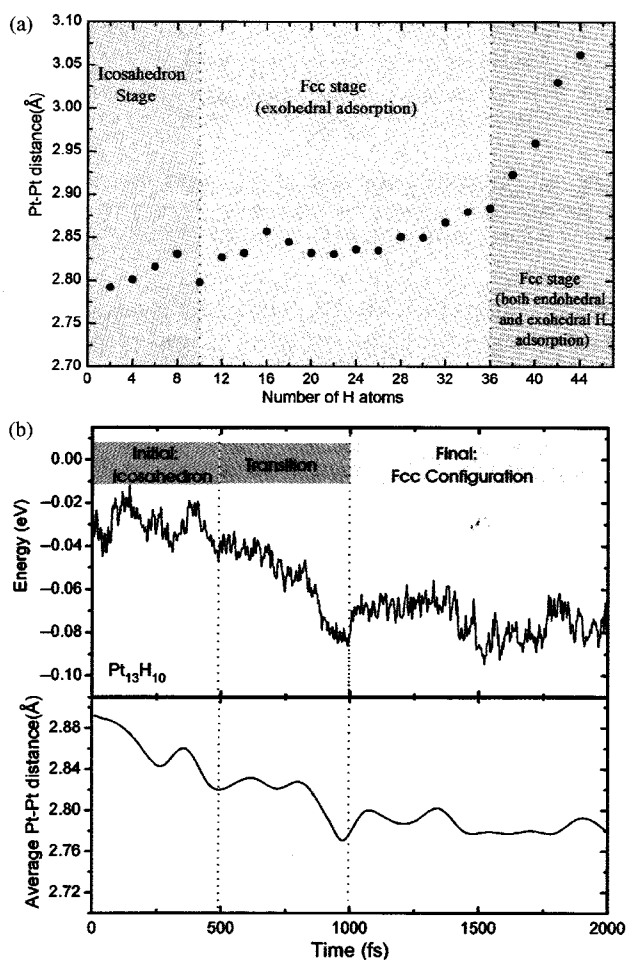

Fig. 3. (a) The average Pt–Pt distances as a function of H coverage; (b) upper panel: energy evolution with time for $Pt_{13}H_{10}$; lower panel: the average Pt–Pt distances of $Pt_{13}H_{10}$.

preferentially and the sequential loading of these sites continues until $n = 36$ as shown in Figure 2(a5). This marks the end of the second stage in Figure 3(a) where all hydrogen atoms are adsorbed at the surface of the Pt_{13} cluster and the average Pt–Pt bond distances fluctuate in a small range of 2.83–2.88 Å for the different numbers of H atoms. The final stage in Figure 3(a) occurs for higher values of H loading. In this stage, the cluster maintains its *fcc*-like structure and the additional H atoms are placed at any of the 6 Vac-H_4 sites. These atoms get pulled into the cluster where they interact with the *core* Pt atom (Figs. 2(a6)–(a8)). The inside H atoms break the connection between the *core* Pt atom and the outer shell Pt atoms, leading to further volume expansion. This is clearly seen in Figure 3(a) where the average Pt–Pt distance increases by about 0.2 Å in going from $n = 36$ to $n = 44$. The phenomenon of H adsorbing inside the surface is quite different with small Pt clusters[32,33] that have no inner atoms. However, it was observed for H adsorption on Pt crystalline surfaces where H atoms diffuse into the Pt lattice after all possible surface sites are saturated.[31]

Figure 4 displays the H_2 dissociative chemisorption energies (ΔE_{CE}), the H sequential desorption energies (ΔE_{DE}), and the average amount of Hirshfeld charge transfer from Pt_{13} to H atoms (ΔQ) with respect to H loading. Similar to smaller Pt clusters,[32,33] there is greater fluctuation in ΔE_{DE} than in ΔE_{CE} due to the energy difference between metal hydrides (see Eq. (2)) which can vary greatly near boundaries where energetically favorable sites become filled. Clear examples may be seen at $n = 24$ where the edge sites are completely filled and at $n = 36$ where the surface sites are completely filled. The dissociative chemisorption energy drops rapidly when H atoms are pulled inside the cluster, however, the charge transfer

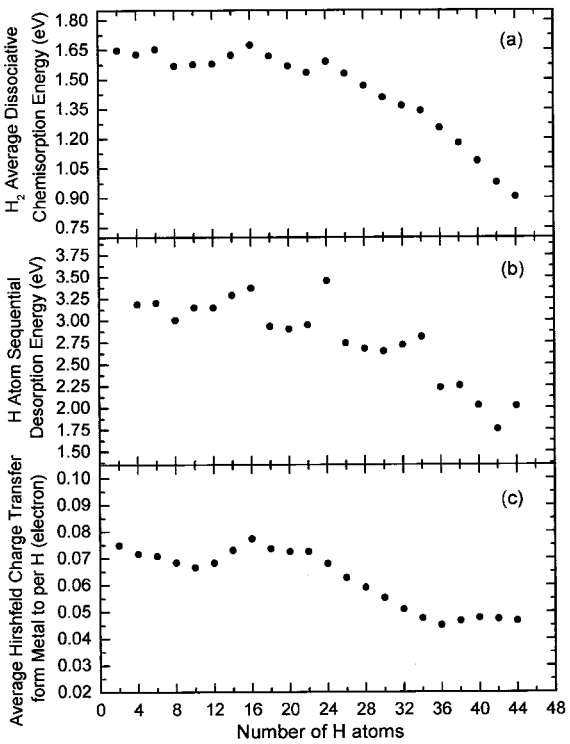

Fig. 4. The calculated (a) dissociative chemisorption energy, (b) sequential desorption energy and (c) average Hirshifeld charge transfer from metal to per H of Pt cluster versus H coverage.

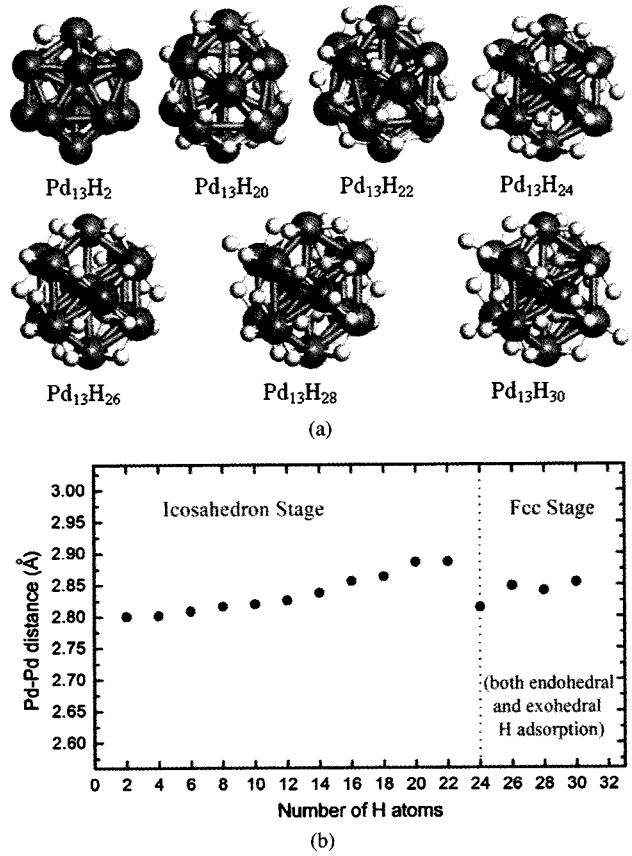

Fig. 5. (a) Optimized structures of H_2 sequential dissociative chemisorption on Pd_{13} cluster. Surface H atoms are shown in white and inside H atoms in yellow; (b) The calculated Pd–Pd distance of $Pd_{13}H_n$.

flattens out. This deviates from the trend found for smaller clusters which showed more correlated behavior between ΔE_{CE} and ΔQ. The calculated values of ΔE_{CE} and ΔE_{DE} at full saturation are 0.90 eV and 2.02 eV, respectively. These values are very close to those found for small Pt clusters[32,33] which suggests that the most important energies are not sensitive to the size or shape of the clusters in the saturation limit.

3.2. H_2 Reactions with Pd_{13} Icosahedral Cluster

Similar to the procedure described above for the Pt_{13} icosahedral cluster, we studied the H_2 dissociative chemisorption and H sequential desorption on the icosahedral Pd_{13} cluster. We allowed for diffusion at low H coverage and searched for the location of the structural transition that was expected to occur with increased loading of H atoms. Again, the edge site of the icosahedral Pd_{13} was identified to be the most active for accepting H atoms at low coverage. The calculated dissociative chemisorption energy is 1.40 eV with an H_2 dissociation and H diffusion barrier of 0.16 eV and 0.07 eV, respectively. The H_2 reactivity is slightly lower than that of Pt_{13}, however, the H diffusion is much more facile, consistent with previous reports.[32–34]

Sequential adding of H atoms to the Pd_{13} cluster was followed as in part A. Selected Pd-hydride structures are displayed in Figure 5. The Pd_{13} cluster maintains its icosahedral structure for higher values of H loading compared to Pt_{13}, and reaches a critical transition point at $n = 22$. The transformation to *fcc*-like structure occurs at $n = 24$ where all the edge sites are filled. Unlike the Pt_{13} cluster, there is no region of *fcc*-like structure where additional H atoms may be sequentially attached to the surface. Any two H atoms that are added to the $Pd_{13}H_{24}$ hydride are pulled inside the cluster surface where they interact with the core Pd atom. Interestingly, our calculations show that the Pd_{13} cluster cannot hold more than 2 H atoms inside the shell. When more H atoms are added to the $Pd_{13}H_{26}$ cluster, they do not enter inside but instead absorb at the $Pd@H_4$ corner sites. This situation differs from that of the Pt_{13} cluster which can hold as many as 6 H atoms at the core site which weakens the Pt–Pt bonds and leads to increased H chemisorption capacity. This conclusion was verified by MD simulations which identified the H saturation point for Pd_{13} to be at $n = 30$, considerably less than the Pt_{13} cluster value of 44. The ratios of hydrogen to metal atoms found here are consistent with those found previously for smaller clusters.[32–34]

Figure 6 displays ΔE_{CE}, ΔE_{DE}, and ΔQ for Pd_{13} with respect to H loading. Again there is strong fluctuation in

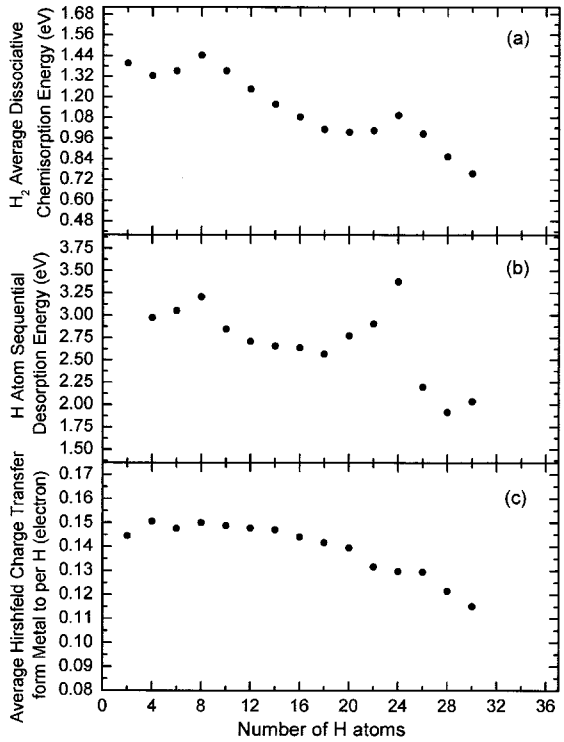

Fig. 6. The calculated (a) dissociative chemisorption energy, (b) sequential desorption energy and (c) average Hirshfeld charge transfer from metal to per H of Pd cluster versus H coverage.

ΔE_{DE} at $n = 24$ where the edge sites are completely filled. The calculated values of ΔE_{CE} and ΔE_{DE} at full saturation were found to be 0.76 eV and 2.04 eV, comparable to those of small Pd clusters.[34] Charge transfer for small Pd clusters was found previously[34] to decrease almost linearly with H coverage. The ΔQ curve given in Figure 6(c) shows mostly flat behavior for the Pd_{13} cluster at small H coverage, but then follows a nearly linear decrease with increased H loading, consistent with the small cluster behavior. It is noteworthy that for both Pt_n and Pd_n clusters with $n < 14$, the saturation values of ΔE_{CE} and ΔE_{DE} do not vary significantly with cluster size and shape. Therefore, it appears that the main difference between these clusters towards H_2 at full saturation of H atoms is that the H capacity of Pt clusters is substantially higher than that of Pd clusters.

3.3. Electronic Properties

Our calculations indicate that Pt_{13} and Pd_{13} bare clusters are magnetic with magnetic moments of 1 μ_B and 4 μ_B, respectively. Upon H_2 dissociative chemisorption on the clusters, the electronic spin states of the bare clusters are altered in the metal hydrides. At full H saturation, the electronic structures of the Pt and Pd hydrides become close-shell due to the fact that the unpaired Pd/Pt d-electrons are now paired with the H-1s electron via d–s orbital overlaps, which annihilates the magnetic moments. This behavior is consistent with our previous findings for small clusters[32–34] but differs from DFT calculations reported by Liu et al.[18] which predicts a non-vanishing magnetic moment for an icosahedral Pt_{13} cluster saturated by 30 surface H atoms likely due to the confined zeolitic bonding environment and inaccessibility by H atoms. Figure 7 displays the calculated density of states (DOS) of both bare and fully H-saturated Pt_{13} and Pd_{13} clusters. Radical changes in the electronic structures upon hydride formation are readily visible. The DOS spectra for the bare metal clusters exhibit typical metal bonding character with the low lying states are dominantly contributed by d-orbitals. For the metal hydrides, the valence bands are contributed mostly by the d-orbitals of the metal atoms and the s-orbitals of H atoms; the conduction bands are primarily contributed by the 5d- and 6s-orbitals of Pt atoms for $Pt_{13}H_{44}$ and by the 4d- and 5s-orbitals of Pd atoms for $Pd_{13}H_{30}$ as H atoms withdraw electrons from the metal atoms. The metallic character of the bare metal clusters exhibited in the DOS spectra is substantially reduced upon the metal hydride formation as the bonding between metal atoms and H atoms is largely of covalent nature.

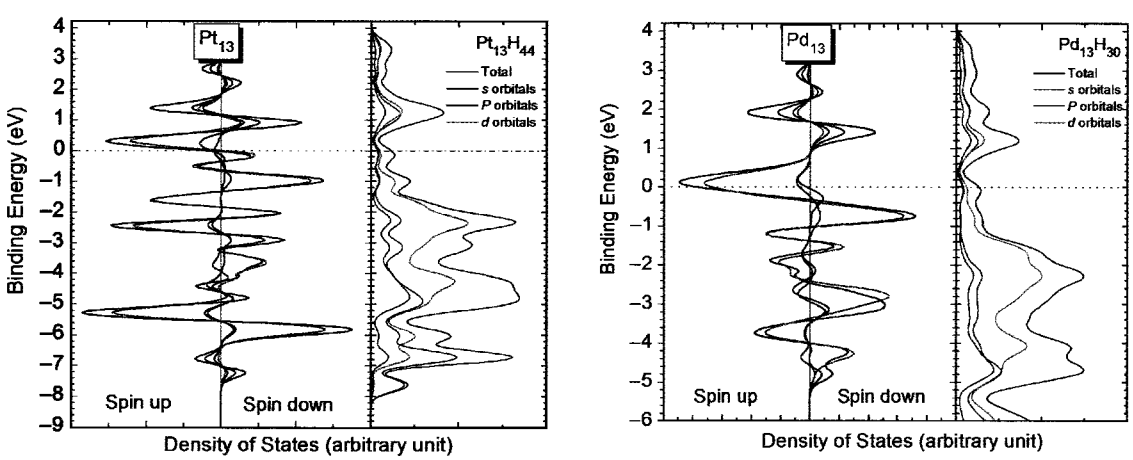

Fig. 7. The calculated density of states of bare and saturated Pt_{13} and Pd_{13} clusters.

4. SUMMARY

Transition metal catalyzed hydrogenation/dehydrogenation reactions are of great scientific and industrial importance and thus have attracted intensive theoretical and experimental interest. In our previous work, we presented DFT studies to quantitatively address the catalytic performance of small Pt and Pd clusters toward H_2 under realistic conditions of constant pressure of hydrogen. We found that the most important properties of the clusters, namely the H_2 dissociative chemisorption energy and the H desorption energy, do not vary significantly with cluster size at full H coverage. In this paper, we extend our investigations to include a slightly larger cluster size of high symmetry to further test the conclusions made previously, and to see whether the catalytic properties of these transition metal clusters exhibit any dependence on the shape of the cluster.

Starting with bare icosahedral Pt_{13} and Pd_{13} clusters, we sequentially added H_2 molecules to the highly symmetric surfaces and computed the adsorption and desorption energies as a function of H coverage. For both Pt_{13} and Pd_{13}, the H_2 dissociative chemisorption energy and H desorption energy at full saturation are comparable with reported values for smaller close-packed clusters despite the structural rearrangement of the clusters themselves. A structural transition from the symmetric icosahedron to an *fcc*-like structure was observed for both Pt_{13} and Pd_{13} prior to H saturation, which provides more active sites for further hydrogen adsorption. H atoms can diffuse into the cluster to interact with the core metal atoms. The number of H atoms that may reside inside Pt_{13} is larger than that of Pd_{13} and allows higher hydrogen capacity. Hirshfeld population analysis shows that electrons flow from metal to H atoms during the hydride formation, which annihilates the magnetism and leads to a close-shell nature of the metal hydrides at full saturation.

Our previous and present studies suggest that some important properties related to the catalytic performance of transition metal clusters may not vary significantly with the particle size or shape. While there is substantial variation in the adsorption and desorption energies for the various shapes and sizes of clusters at low H coverage, these energies lie within a narrow range when the clusters reach full H saturation. Therefore, under practical experimental conditions of constant H_2 pressure, it appears that the energetic properties are dependent primarily on the available surface atoms of metal which can be accessed by H atoms. This observation should be very helpful in the design of novel catalysts for real industrial applications.

It is important to note that the present studies included only exceedingly small metal cluster size. Catalyst particles used in practice is substantially larger than the subnano clusters used in our calculations. These particles are dispersed onto support materials. To gain complete understanding of the catalytic activities, further studies on the fundamental properties of supported larger clusters are needed.

Acknowledgment: This work is supported by the National Natural Science Foundation of China under Grant No. 20703040.

References

1. R. L. Augustine, Heterogeneous Catalysis for the Synthetic Chemist, Marcel Dekker Inc., New York **(1995)**.
2. T. E. Felter, S. M. Foiles, M. S. Daw, and R. H. Stulen, *Surf. Sci. Lett.* 171, L379 **(1986)**.
3. P. S. Cremer, X. Su, Y. R. Shen, and G. A. Somorjai, *J. Am. Chem. Soc.* 118, 2942 **(1996)**.
4. S. F. Parker, C. D. Frost, M. Telling, P. Albers, M. Lopez, and K. Seitz, *Catal. Today* 114, 418 **(2006)**.
5. K. Christmann, G. Ertl, and T. Pignet, *Surf. Sci.* 54, 365 **(1976)**.
6. B. E. Nieuwenhuys, *Surf. Sci.* 59, 430 **(1976)**.
7. M. K. Bowman and L. Kevan, Time Domain Electron Spin Resonance, Wiley, New York **(1979)**.
8. W. Palczewska, Hydrogen Effects in Catalysis, Marcel Dekker, New York **(1988)**.
9. L. K. Verheij, M. B. Hugenschmidt, A. B. Anton, B. Poelsema, and G. Comsa, *Surf. Sci.* 210, 1 **(1989)**.
10. Ş. C. Bădescu, P. Salo, T. Ala-Nissila, S. C. Ying, K. Jacobi, Y. Wang, K. Bedüftig, and G. Ertl, *Phys. Rev. Lett.* 88, 136101 **(2002)**.
11. L. J. Richter and W. Ho, *Phys. Rev. B* 36, 9797 **(1987)**.
12. L. K. Verheij and M. B. Hugenschmidt, *Surf. Sci.* 324, 185 **(1995)**.
13. S. Horch, H. T. Lorensen, S. Helveg, E. Laegsgaard, I. Stensgaard, K. W. Jacobsen, J. K. Nørskov, and F. Besenbacher, *Nature* 398, 134 **(1999)**.
14. A. P. Graham, A. Menzel, and J. P. Toennies, *J. Chem. Phys.* 111, 1676 **(1999)**.
15. H. Okuyama, T. Nakagawa, W. Siga, N. Takagi, M. Nishijima, and T. Aruga, *J. Phys. Chem. B* 103, 7876 **(1999)**.
16. S. Buckart, G. Gantefor, Y. D. Kim, and P. Jena, *J. Am. Chem. Soc.* 125, 14205 **(2003)**.
17. M. K. Oudenhuijzen, J. A. van Bokhoven, J. T. Miller, D. E. Ramaker, and D. C. Koningsberger, *J. Am. Chem. Soc.* 127, 1530 **(2005)**.
18. X. Liu, H. Dilger, R. A. Eichel, J. Kunstmann, and E. Roduner, *J. Phys. Chem. B* 110, 2013 **(2006)**.
19. H. Jiang, H. Yang, R. Hawkins, and Z. Ring, *Catal. Today* 125, 282 **(2007)**.
20. P. J. Feibelman and D. R. Hamann, *Surf. Sci.* 182, 411 **(1987)**.
21. R. A. Olsen, G. J. Kroes, and E. J. Baerends, *J. Chem. Phys.* 111, 11155 **(1999)**.
22. K. Nobuhara, H. Nakanishi, H. Kasai, and A. Okiji, *J. Appl. Phys.* 88, 6897 **(2000)**.
23. G. Papoian, J. K. Nørskov, and R. Hoffmann, *J. Am. Chem. Soc.* 122, 4129 **(2000)**.
24. G. W. Watson, R. P. K. Wells, D. J. Willock, and G. J. Hutchings, *J. Phys. Chem. B* 105, 4889 **(2001)**.
25. K. Nobuhara, H. Kasai, H. Nakanishi, and A. Okiji, *J. Appl. Phys.* 92, 5704 **(2002)**.
26. K. Nobuhara, H. Kasai, W. A. Diño, and H. Nakanishi, *Surf. Sci.* 566–568, 703 **(2004)**.
27. K. Balasubramanian, *J. Chem. Phys.* 94, 1253 **(1991)**.
28. D. Dai, D. W. Liao, and K. Balasubramanian, *J. Chem. Phys.* 102, 7530 **(1995)**.
29. Y. Okamoto, *Chem. Phys. Lett.* 405, 79 **(2005)**.
30. Y. Okamoto, *Chem. Phys. Lett.* 429, 209 **(2006)**.
31. P. Légaré, *Surf. Sci.* 559, 169 **(2004)**.
32. L. Chen, A. C. Cooper, G. P. Pez, and H. Cheng, *J. Phys. Chem. C* 111, 5514 **(2007)**.

33. C. Zhou, J. Wu, A. Nie, R. C. Forrey, A. Tachibana, and H. Cheng, *J. Phys. Chem. C* 111, 12773 (**2007**).
34. C. Zhou, S. Yao, J. Wu, R. C. Forrey, L. Chen, A. Tachibana, and H. Cheng, *Phys. Chem. Chem. Phys.* 10, 5445 (**2008**).
35. A. Nie, J. Wu, C. Zhou, S. Yao, C. Luo, R. C. Forrey, and H. Cheng, *Int. J. Quantum Chem.* 107, 219 (**2007**).
36. C. Luo, C. Zhou, J. Wu, T. J. D. Kumar, N. Balakrishnan, R. C. Forrey, and H. Cheng, *Int. J. Quantum Chem.* 107, 1632 (**2007**).
37. J. P. Perdew, J. A. Chevary, S. H. Vosko, K. A. Jackson, M. R. Pederson, D. J. Singh, and C. Fiolhais, *Phys. Rev. B* 46, 6671 (**1992**).
38. J. P. Perdew and Y. Wang, *Phys. Rev. B* 45, 13244 (**1992**).
39. T. A. Halgren and W. N. Lipscomb, *Chem. Phys. Lett.* 49, 225 (**1977**).
40. B. Delley, *J. Chem. Phys.* 92, 508 (**1990**).
41. B. Delley, *J. Chem. Phys.* 113, 7756 (**2000**).

Received: 5 August 2008. Accepted: 15 August 2008.